Journal of the Australian Ceramic Society (2021) 57:1085–1095
https://doi.org/10.1007/s41779-021-00607-z

RESEARCH

The effect of graphene+boron nitride/ZnO-based hybrid nanocomposites: synthesis, electrical, optical properties

Ömer Güler[1] · Seval Hale Güler[1] · Öyküm Başgöz[1] · I.S. Yahia[2,3,4]

Received: 2 November 2020 / Revised: 5 April 2021 / Accepted: 22 April 2021 / Published online: 8 May 2021

Abstract

In this study, nanocomposites ZnO-doped graphene+boron nitride nanosheets (BNNS) were produced, and their electrical and optical properties were investigated. The graphene+BN nano-hybrid layer used as a reinforcement element was synthesized using a liquid-phase exfoliation method. TEM images support the nanosheet's structure of the graphene and boron nitride. ZnO produced by sol-gel showed nanoscale spherical particles, while the commercial ZnO showed the micrometer scale with rod-like and hexagonal shapes. Composite materials were provided by reinforcing this reinforcement element into ZnO matrices, which were commercially available and were produced using the sol-gel procedure at different ratios. To compare the results, the BN nanosheets were synthesized using liquid-phase exfoliation. Using the same method, samples for comparison were produced by reinforcing these nano-hybrid sheets into the commercially available ZnO matrix and the sol-gel synthesized ZnO matrix. A limited increase was shown for the 0.1 wt% and 0.5 wt% in the nanocomposites' electrical conductivity ratios, along with the rise of the graphene + BN nano-hybrid sheet. The E_g values of the as-produced nanocomposites first decreased and then increased as the reinforcement ratio increased. The bandgap changing for all reinforcing types exhibits similar characters. The studied materials can be used in wide-scale electronic and optoelectronic devices, environmental, biomedical, and catalytic/photocatalytic activities.

Keywords Graphene/ZnO · Boron nitride/ZnO · Nanocomposites · Optical and electrical analysis · Bandgap · Conduction mechanisms

Introduction

Graphene, which is 2D carbon nanostructures, refers to a single layer of graphite comprised of multiple layers stacked on top of one another. Graphene is a material that has attracted the attention of many researchers ever since its discovery. Since being a two-dimensional material, graphene has numerous features, such as its enormous mechanical strength, excellent thermal and mechanical stability, and extremely high carrier mobility. It attracts such attention [1–4]. Thanks to these properties, graphene would play an essential part in developing advanced electronic and optoelectronic devices.

Nevertheless, graphene should also be used to create semiconductors because there are no significant band gaps in graphene. After all, the current cannot be deactivated before the electrons begin fluid. Therefore, massless particles, which are one of graphene's most significant properties, can become its most disadvantageous feature in specific electronic applications [5–7]. Thus, at the atomic level, graphene is thin, and its electronic band structure has a low density at the Dirac point stage. Hence, the transfer of carriers between the graphene and the semiconductor reduces the Schottky diode's barrier height using this material.

Therefore, the performance of Schottky diodes using a graphene-semiconductor pair is limited [4, 8, 9]. This negative

✉ Ömer Güler

✉ I.S. Yahia
dr_isyahia@yahoo.com; isyahia@gmail.com; ihussein@kku.edu

[1] Metalurgical and Material Engineering Department, Engineering Faculty, Mersin University, Mersin, Turkey

[2] Research Center for Advanced Materials Science (RCAMS), King Khalid University, P.O. Box 9004, Abha 61413, Saudi Arabia

[3] Department of Physics, Faculty of Science, Advanced Functional Materials & Optoelectronic Laboratory (AFMOL), King Khalid University, P.O. Box 9004, Abha, Saudi Arabia

[4] Nanoscience Laboratory for Environmental and Biomedical Applications (NLEBA), Semiconductor Lab., Department of Physics, Faculty of Education, Ain Shams University, Roxy, Cairo 11757, Egypt

situation can be eliminated by placing an insulating layer between the graphene and the semiconductor. The insulation layer's ideal form to be used graphene-based semiconductors would be boron nitride nanosheets (BNNS). BNNSs has a bandgap of 5.9 eV. Moreover, they also have a high degree of chemical stability, high transparency, and flexibility [10, 11]. Thanks to its such properties, BNs could be used as dielectric layers in flexible electronics [12].

In recent studies, it was seen that metal oxides, which were reinforced by boron nitrides, display excellent photocatalytic activities [13, 14]. BN nanosheets can behave as enabling matrix and co-material without metal that increases the photocatalytic efficacy and stableness of nanostructured semiconductors; the promotion of this change is clarified by segregation of electrons and holes in the photocatalytic reaction [15, 16].

In this study, both hexagonal BN and graphite powders were evenly mixed, and graphene+BN nano-hybrid sheets were synthesized using liquid-phase exfoliation. The resulting nano-hybrid sheets have been doped into a commercially available ZnO matrix and another ZnO matrix produced for comparative study by the sol-gel technique. The materials obtained were analyzed in their electrical and optical properties. It is important to mention for the Schottky diodes that it is a complicated process to place the BN nanosheets as a single layer between the semiconductor and the graphene. This research is targeted at present the change in characteristics of the as-produced nanocomposite as a consequence of the random dispersion of the graphene + BN nano-hybrid sheets inside the ZnO matrix produced by a straightforward method.

Experimental details

In this study, the nanocomposites of the ZnO-graphene+boron nitride nano-hybrid sheet were synthesized to form two separate groups. The ZnO matrix caused the difference between the two groups. While the first group's matrix element was a commercially available ZnO, while the second group, on the other hand, was the ZnO synthesized using the sol-gel method. Among both groups, graphene+boron nitride nano-hybrid sheet mixtures were used as a reinforcement element. Additionally, the BN nanosheets were also manufactured for comparison purposes. The BN nanosheets were likewise reinforced into the ZnO matrix.

The synthesize of graphene+boron nitride nanosheets and boron nitride nanosheets using liquid-phase exfoliation method

Hexagonal boron nitride (h-BN) (Merck, 99.5%) and hexagonal graphite (h-G) (Merck, 99.5%) powders were dried in a vacuum furnace at a temperature equal to 75 °C for 2 h to remove any present moisture. The dehumidified h-G and h-BN were then mixed in equal amounts by weight. The powders were blended for 12 h into concentrated H_2SO_4 and HNO_3 saturated acid to produce an intercalated hybrid compound. During the process, the uniform intercalation of all graphite and boron nitride particles was achieved by blending the hybrid mixture with magnetic agitation. The powders have been refined and washed with distilled water until a neutral pH is obtained after the mixing. The resulting treated powders were dried in the vacuum furnace for 12 h. Then, a powder mixture was then heated to 800 °C to extend the layers' distance. The powders obtained through this process were then exfoliated with the aid of an ultrasonic homogenizer in *N*,*N*-dimethylformamide (DMF). In a 1-h using multiple frequency ultrasonic homogenizer, the solution for extended powder blends and DMF was preserved. Then, the DMF was removed by centrifuging the mixture for 8 h at 5000 rpm. The same method described was used for synthesizing BN nanosheets above.

Nano-ZnO synthesis

ZnO was produced using the sol-gel technique before the production of ZnO nanocomposites. The ZnO production initiator was 11 g of zinc acetate dihydrate in sol-gel dependent on hydrolysis and molecular precursor condensation. Twenty-five milliliters of ethylene glycol monomethyl ether, a suitable solvent for zinc acetate dihydrate, was mixed at 60 °C using a magnetic stirrer/hotplate. The solution was then added 25 ml of ethanolamine, where gelation was observed after stirring at 60 ° C for a while and then calcined for 8 h at 600 °C.

Production of ZnO-graphene+boron nitride nanosheet nanocomposites

Graphene+boron nitride nano-hybrid sheet mixed in 0.1 wt%, 0.5 wt%, and 1 wt% of commercially available pure ZnO (Metal Oksit Co., 99.5%) and sol-gel-produced ZnO were added. Therefore, the nano-hybrid nitride mixtures, weighted accordingly, were dispersed in absolute alcohol with an ultrasonic homogenizer. ZnO powders were then added to the alcohol and mixed until inappropriate evaporation quantities resulting powder blend was pasted under 600 MPa and then sintered for 1 h at 700°C in an argon-based environment. The production of nanocomposites of ZnO-BN nanosheets was identical to the creation of nanocomposites described above.

A code was given for the as-produced samples. Table 1 shows the as-synthesized samples' codes and the weight percentages of the ZnO matrix/reinforcing elements. All synthesized samples were encoded as H_x and SH_x. While H_x represents the commercially available ZnO-doped graphene+boron nitride nano-hybrid sheet reinforced samples, SHx represents

Table 1 The sample codes and weight percentages of ZnO matrix/graphene-BN nano-hybrid sheets

Sample codes	Matrix	Reinforcement names	Doped in wt%
C	Commercial ZnO	-	0
S	Sol-gel ZnO	-	0
H_1	Commercial ZnO	Graphene-BN nano-hybrid sheets	0.1
H_2	Commercial ZnO	Graphene-BN nano-hybrid sheets	0.5
H_3	Commercial ZnO	Graphene-BN nano-hybrid sheets	1
SH_1	Sol-gel ZnO	Graphene-BN nano-hybrid sheets	0.1
SH_2	Sol-gel ZnO	Graphene-BN nano-hybrid sheets	0.5
SH_3	Sol-gel ZnO	Graphene-BN nano-hybrid sheets	1
B_1	Commercial ZnO	BN nanosheets	0.1
B_2	Commercial ZnO	BN nanosheets	0.5
B_3	Commercial ZnO	BN nanosheets	1
SB_1	Sol-gel ZnO	BN nanosheets	0.1
SB_2	Sol-gel ZnO	BN nanosheets	0.5
SB_3	Sol-gel ZnO	BN nanosheets	1

the graphene+boron nitride nano-hybrid sheet mixture samples with ZnO matrix synthesized using the sol-gel method.

Devices and measurements

The microstructures of nano-hybrid surface samples are studied with a transmittal electron microscope (TEM) (JEOL Jem 2100F). Tests have been performed with the JEOl JSM-7001F scanning electron microscopy (SEM).

The nanocomposites' electrical conductivity measurements were carried out using a dual probing method utilizing a Keithley 6517A Electrometer/High-resistance meter device. A schematic diagram of the DC electrical conductivity was given in Fig. 1.

Optical measuring was conducted using the Shimadzu UV-3600, UV-Vis spectrophotometer between 250 and 1200 nm to record the diffused reflective spectrum. In comparison with the $BaSO_4$ baseline, the diffuse reflectance has been measured.

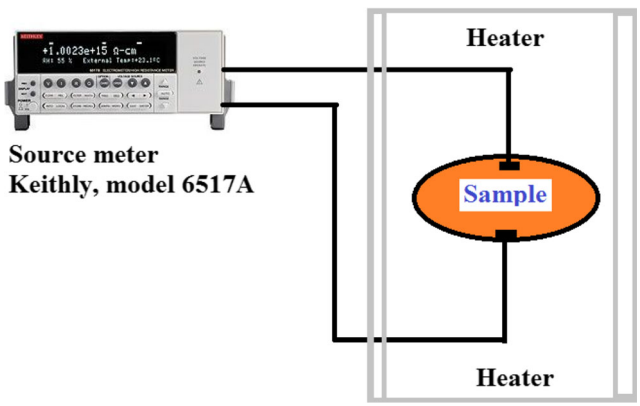

Fig. 1 Schematic diagram of the DC electrical conductivity for the studied nanomaterials

Results and discussion

Study of the graphene+BN nano-hybrid sheet and BN nanosheets microstructure

The graphene+BN nano-hybrid sheets and the BN nanosheets reinforced with the ZnO matrix were synthesized using the liquid phase exfoliation method. This method's basic principle is based on separating the hexagonal graphite layers or hexagonal boron nitride composed of multi-stacked layers. The hexagonal graphite and hexagonal boron nitride with the stacked layers were connected via weak Van- der-Waals bonds. Some of the solvents' atoms to be placed between these layers will cause these bonds to break, thus leading the layers to detach, although different solutions can be used in the production of nanolayers using the liquid-phase exfoliation method. DMF was preferred in this study.

The TEM images from the nano-hybrid sheet graphene+BN and the liquid stage exfoliation process were shown in Fig. 2a, b. In Fig. 2a, two different types of layers could be mentioned. One of these layers had a more uniform and had an almost circular geometry. The other layer had a more irregular structure. The other irregular-shaped structures belonged to the graphene layers. In many parts of the structure, it can be asserted that graphene layers and BN nanosheets overlap. Also, the width of the sheets produced was above 200 nm. Figure 2b shows the TEM image of the BN nanosheet. Upon looking at this image in Fig. 2b, the BN nanosheets had a circular-like geometry,

Only the TEM images will be given to characterize the graphene + BN nano-hybrid sheet and BN nanosheets in this study. Further characterization techniques have been extensively covered in our group's previously reported studies, including these layers [17–20].

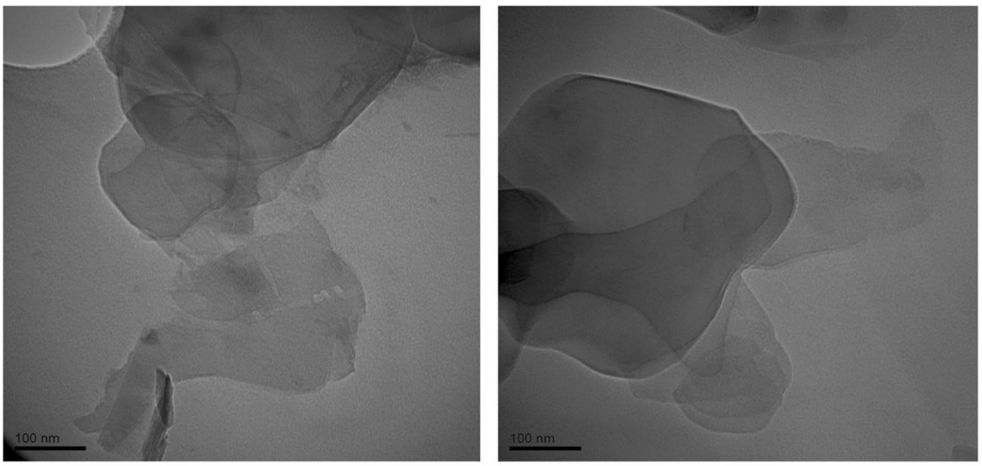

Fig. 2 **a**, **b** TEM images of **a** graphene-BN nanosheets mixtures and **b** BN nanosheets

Study of the ZnO-graphene+BN nano-hybrid sheets nanocomposites microstructure

A total of 14 samples were featured in this study using SEM images for each studied sample group, but the sample numbers are too much, so SEM images of two samples from each group were given. Figure 3 shows the SEM images of samples H_1, H_2, SH_1, SH_2, B_1, B_2, SB_1, and SB_2

All the as-produced nanocomposites were in powder form. During the production process, the nano-lays used as a strengthening matter were covered by the ZnO matrix; no sound pictures could be made from the bulk samples' surfaces. SEM images have therefore been taken from sample sections. In all the samples, the ZnO matrix and reinforcements surrounding the layers were integrated into the matrix. In the samples in which the commercially available ZnO was used, the matrix particles' dimensions were at the micrometer level, and the particles had rod-like and hexagonal shapes. On the other hand, in the samples in which the sol-gel-produced ZnO was used, the particle size was at the nanometer level, and the particles themselves had a spherical form.

The electrical properties of ZnO-graphene+BN nano-hybrid sheets nanocomposites

Figure 4 shows the DC electrical conductivity plots for the samples studied, and the temperature varies from room temperature to 150 °C. Figure 4a shows the electrical conductivity changing graph of samples containing the commercially ZnO matrix, whereas Figure 4b shows the DC electrical connectivity plots of the samples containing the sol-gel-synthesized ZnO matrix. Figure 4c–f shows comparatively the samples with the same reinforcement ratio from each group. Samples with the graphene + BN nano-hybrid sheets were more electrical conductivity than those of samples reinforced only with the BN nanosheets. The high conductivity of H-group samples was due to the graphene layers. ZnO matrix was an excellent electron donor material, and the graphene layers embedded in the ZnO matrix were an excellent electron acceptor. The DC electrical conductivity of samples containing only the BN nanosheets (i.e., B or SB group samples) as a reinforcing material was lower than H-group samples. This was an expected result. This is because BN is an excellent insulating material. The typical results of all of the samples were that:

(1) The DC conductivity of specimens containing commercially available pure ZnO was higher than the samples containing the as-produced sol-gel ZnO matrix for the same reinforcement ratio. Even the DC electrical conductivity value of the SH-group samples was identical to that of the samples containing sol-gel-synthesized ZnO, even at a reinforcement ratio of 0.1 wt% and 0.5 wt%, respectively. However, this is not the case among samples with the ZnO matrix commercially available. The DC electrical conductivity value of the enhanced graphene+BN nano-hybrid sheets in terms of reinforcement value was increased.

(2) The DC electrical conductivity of the B_1-group samples was higher than those of the SH_1-group samples. The same was also present between both the B_2 and SH_2 samples up to a certain temperature. However, the same was not present between the B_3 and SH_3 samples. This is because the graphene in the SH_3 sample exceeded the conductivity by a certain amount.

(3) In the samples with a sol-gel-synthesized ZnO matrix, significant increases in the DC electrical conductivity were observed with the increase of temperature. These increment increase rates in the conductivity were not observed at this level in samples with a commercially available ZnO matrix. This suggested that the sol-gel produced ZnO matrix samples were profoundly affected by the surrounding raising of temperature.

(4) In the SB- and B-group samples, the ZnO matrix started to show an insulating character with the increasing amount of BN nanosheets.

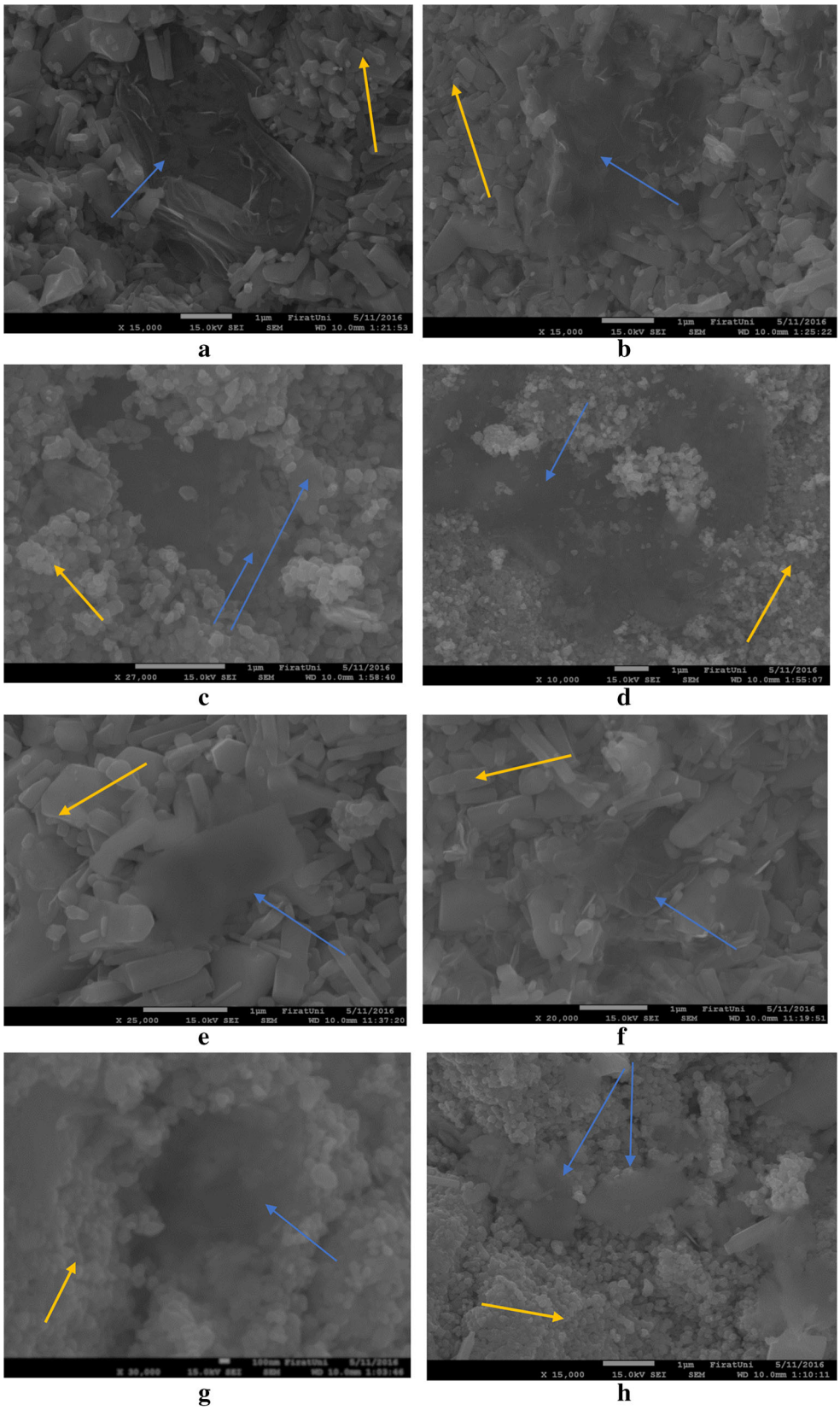

Fig. 3 **a**–**h** SEM images of **a** H_1, **b** H_2, **c** SH_1, **d** SH_2, **e** B_1, **f** B_2, **g** SB_1, **h** SB_2 nanosamples (yellow arrows, matrix; blue arrows, nanosheets)

Both the H_3 and SH_3 coded samples were reinforced with the graphene-BN nano-hybrid sheet at the ratio of 1 wt%. This signified that the graphene nanolayers were present at the ratio of 0.5 wt% within the nanocomposite structure. However, in

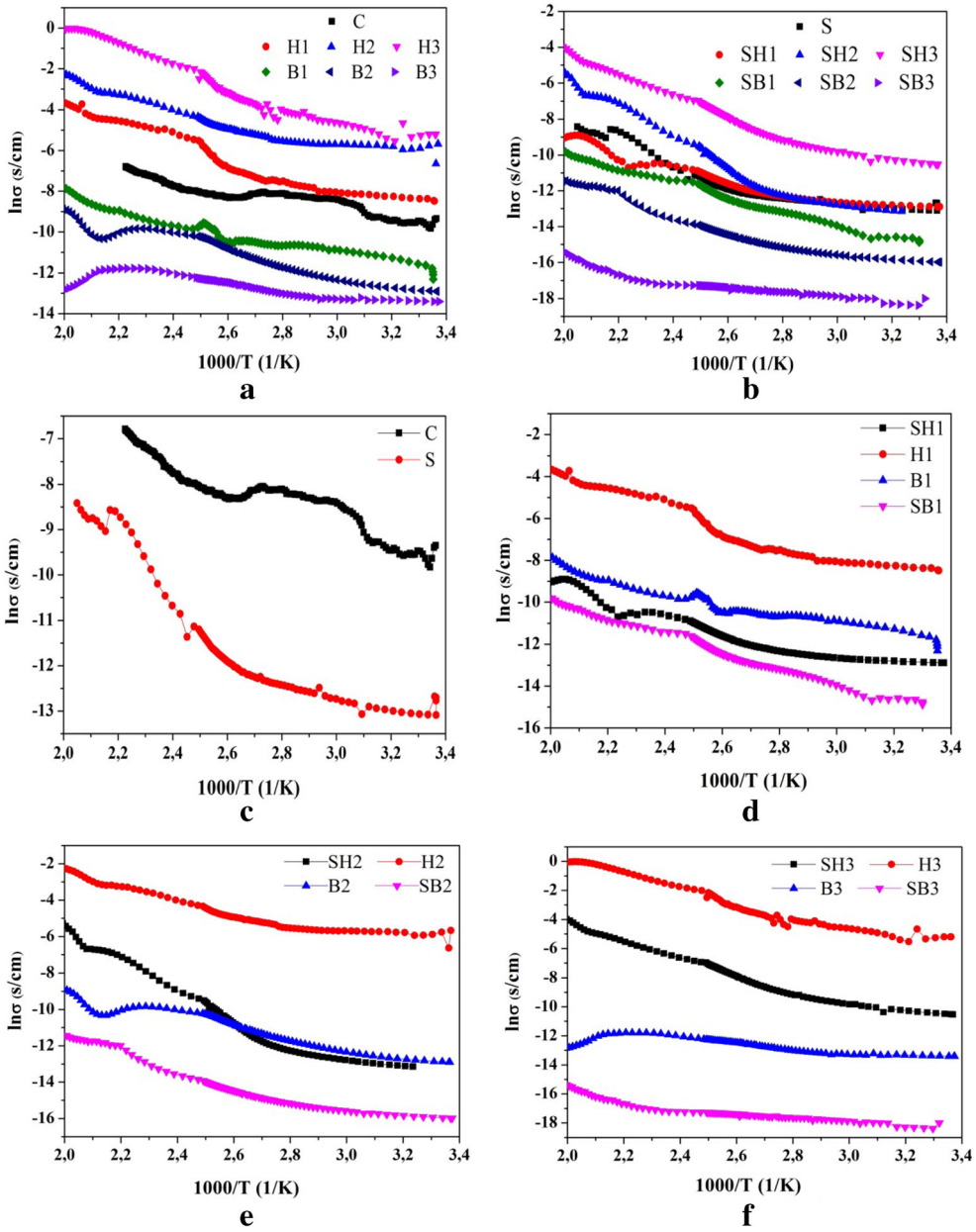

Fig. 4 **a**–**f** The DC electrical conductivity plots of **a** commercial ZnO matrix, **b** sol-gel ZnO matrix, **c** pure ZnO samples, **d** all nanocomposites having the 0.1 wt% nanosheets, **e** all nanocomposites having 0.5 wt% nanosheets, **f** all nanocomposites having 1 wt% nanosheets

the comparative studies with the previously reported data [21–23], the increase in DC electrical conductivity of ZnO matrix composites reinforced with either carbon nanotubes at the same ratio of different carbon nanostructures was higher than those obtained in this study. In the study of Güler et al. [22], the electrical conductivity of the ZnO-CNT composite was 4×10^{-3} S/cm for 1 wt% CNT reinforcing. In different work [23], the ZnO-CNT composite's electrical conductivity was measured 2.83×10^{-2} S/cm for excessive CNT amount (5 wt%).

The fact that the increase in DC electrical conductivity of the samples reinforced with graphene+BN nano-hybrid sheets was lower in this study in comparison with previous studies, which can be explained as follows [24]:

(1) All the nanolayers manufactured using liquid-phase exfoliation techniques were uniform and of various thicknesses. This, in turn, negatively affected the increase in the DC electrical conductivity of the nanocomposites. Marinho et al. [24] reported that many particle contacts effectively increased the DC electrical conductivity of carbon-based materials. This study stated that the compact pressure was sufficient and can control the conductivity by slight pressure [24].

(2) The graphene and BN nanosheets were randomly spread distributed in the ZnO matrix, and the two nanolayers even overlapped in some areas. The DC electrical conductivity of the nanocomposites was relatively limited due to the BN nanosheets.

Depending on the curves' line segments, the studied samples' electrical activation energy can be calculated

individually for these straight lines. The DC electrical conductivity showed a straight portion with electrical activation energy named as ΔE_a The DC electrical conductivity was calculated according to the relation [25–27]:

$$\sigma = \sigma_o \exp\left(-\frac{\Delta \mathrm{Ea}}{\mathrm{kT}}\right), \quad (1)$$

All the symbols are well known [25–27]. Table 2 for all prepared samples shows the calculated activation energy. For pure samples, ΔE_a value of commercial ZnO (C sample) is higher than sol-gel ZnO (S sample). Except for SB groups samples, ΔE_a values increase by increasing reinforcing ratios in all other group samples, but ΔE_a values of SB group samples decrease by increasing reinforcing ratios. In previous studies, ΔE_a value of ZnO decrease by increasing CNT ratios [23], but ΔE_a value of ZnO increased by increasing of graphene nanolayer ratios in different a work [28].

Optical properties of ZnO-graphene+BN nano-hybrid sheets nanocomposites

Figure 5 shows the diffused reflectance spectra versus the wavelength of the studied ZnO-graphene + BN nano-hybrid sheets nanocomposites. Figure 5a shows reflectance plots of the samples containing the commercially ZnO matrix, whereas Fig. 5b shows reflectance plots of the samples containing the sol-gel-synthesized ZnO matrix, while Fig. 5c–f shows comparative examples with the same reinforcement ratio. It was observed that the reflectance showed a sharp increase in its value in the wavelength region from 360 to 370 nm for all designed samples for H, SH, B, and SB samples.

Table 2 Electrical activation energy ΔE_A of all nanocomposites

Name of the samples	Activation energy (ΔE_A), (eV)
C	0,439
S	0.132
H_1	0.247
H_2	0.368
H_3	0.445
SH_1	0.183
SH_2	0.255
SH_3	0.354
B_1	0.111
B_2	0.181
B_3	0.204
SB_1	0.308
SB_2	0.279
SB_3	0.1

Whereby the samples with codes C, S, H_1, H_2, H_3, SH_1, SH_2, SH_3, B_1, B_2, B_3, SB_1, SB_2, and SB_3 had a strong reflective characteristic in it in the wavelength regions 363–412, 372–440, 366–450, 368–425, 370–420, 372–435, 372–445, 373–430, 371–463, 372–470, 365–420, 372–473, 373–440, and 374–450 nm, respectively.

Optical absorption analysis was used to assess the bandgap with diffused reflectance measurements of the graphene+BN nano-hybrid nanosheets doped ZnO matrix. The diffused reflectance values were transformed into the absorbance values using the Kubelka-Munk function [29]. Kubelka-Munk theory is generally used to assess the diffuse reflection spectra acquired in non-absorbing samples. The formula Kubelka-Munk can be expressed using [29]:

$$F(R) = (1-R)^2/2R, \quad (2)$$

All symbols are well known [29]. The following equation was used to transform Kubelka-Munk function F(R) values to the linear absorption coefficient (α):

$$\alpha = \frac{F(R)}{t} = \frac{\text{Absorbance}}{t}, \quad (3)$$

All symbols are well known [29]. It is estimated that ZnO has a direct optical bandgap. Thus, optical band gaps of ZnO-graphene+BN nano-hybrid sheets nanocomposites can be determined using the following equation [30]:

$$\alpha h\upsilon = C(\mathrm{h}\upsilon - Eg)^{1/2}, \quad (4)$$

All symbols are well known [30]. The $(ah\upsilon)^2$ graphs against $h\upsilon$ are plotted in Fig. 6a–f with the aid of the absorption coefficient values using the optical absorbance Eqs. (2–4) [25, 26, 28]. The intercept values with the x-axis ($h\upsilon$ axis= zero) yield the energy bandgap values for ZnO-graphene + BN nano-hybrid sheets nanocomposites. Table 3 shows the values of the calculated bandgap for all synthesized samples. The energy gap of the composites was in the range of 3.14–3.28 eV.

For all group samples, E_g values decrease in 0.1 wt% reinforcing ratios, but for 0.5 and 1 wt% reinforced samples in all groups, E_g values increase by increasing reinforcing ratios. For E_g, their values of all nanocomposites are higher than pure samples. It is reported that the E_g value of ZnO decreases with increasing graphene amounts [31]. Besides, it is seen that The ZnO-graphene nanocomposites exhibit high photocatalytic properties, and therefore, Graphene-ZnO nanocomposites are an extreme industrial photocatalytic candidate [32]. Boron nitride nanosheet reinforced some semiconductors exhibit successful results in photocatalytic applications. Between BN and semiconductor occur highly active bondings, and these bondings make an extended wavelength range from UV- to visible light spectrum [33].

In previous literature studies, few studies have investigated the synergistic effect of graphene and BNNS on any matrix.

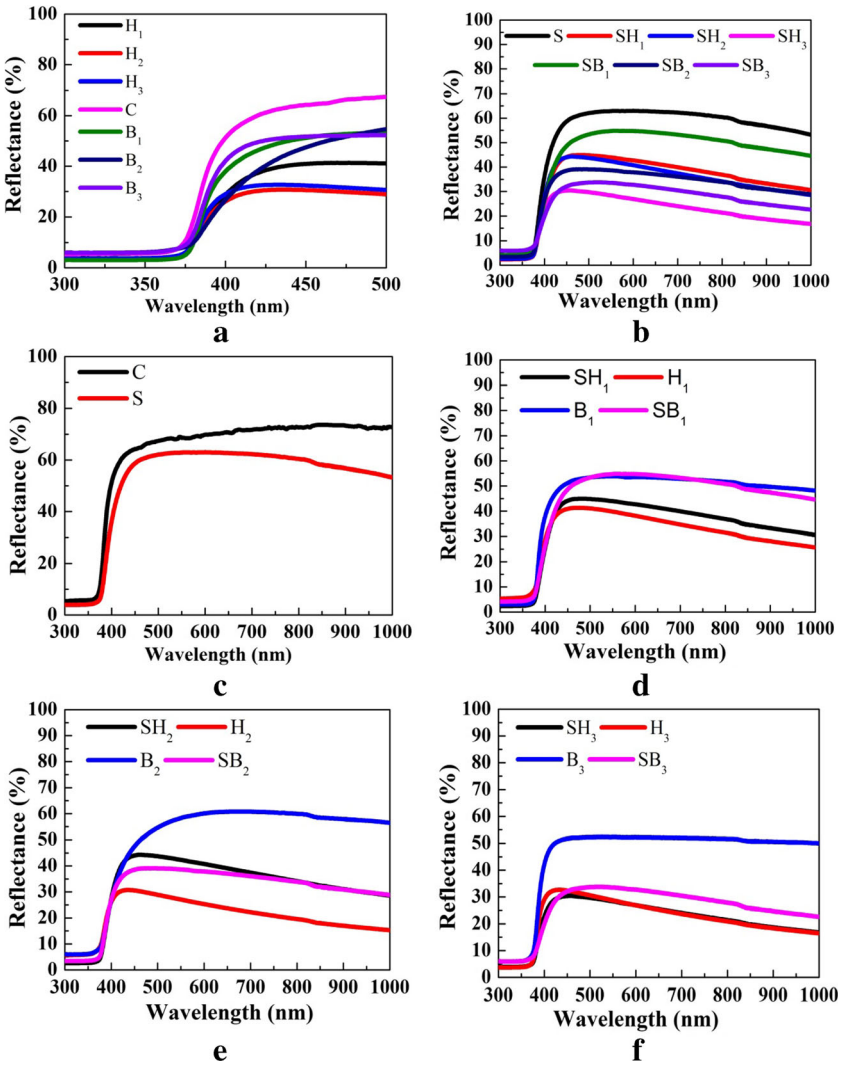

Fig. 5 **a-f** The diffused reflectance versus the incident wavelength of **a** commercial ZnO matrix, **b** sol-gel ZnO matrix, **c** pure ZnO samples, **d** all nanocomposites having 0.1 wt% nanosheets, **e** all nanocomposites having 0.5 wt% nanosheets, **f** all nanocomposites having 1 wt% nanosheets

Table 3 Optical bandgap (E_g) of all nanocomposites

Name of the samples	Optical bandgap, E_g, (eV)
C	3.28
S	3.26
H_1	3.11
H_2	3.20
H_3	3.26
SH_1	3.14
SH_2	3.22
SH_3	3.23
B_1	3.16
B_2	3.18
B_3	3.22
SB_1	3.16
SB_2	3.21
SB_3	3.22

Guo et al. worked on developing highly thermally conductive dielectric nanocomposites by taking advantage of the synergistic effect of graphene and BNNS [34]. Guo et al. made the sandwich structure from matrix, graphene, and BNNS in their work. Consequently, the micro-sandwich nanocomposite provides a high dielectric constant of ≈579, a high energy density, and excellent thermal conductivity. In our study, graphene and BNNS production and the liquid phase exfoliation method enabled the graphenes and BNNS to overlap and form a micro-sized sandwich structure. The TEM picture in Fig. 2a also shows this situation.

Sajjad et al. examined the graphene/BNNS/SiO_2 and graphene/BNNS/metal heterostructure under direct current in their study [35]. The current vs voltage I(V) data for the G/BNNS/Metal devices show Schottky barrier characteristics with very low forward voltage drop, Fowler-Nordheim behavior, and 10^{-4} Ω/sq (this value is 10^6 in graphene/BNNS/SiO_2 structure). They reported that this result is ascribed to the combination of fast electron transport within graphene grains and out-of-plane tunneling in BNNS that circumvents grain

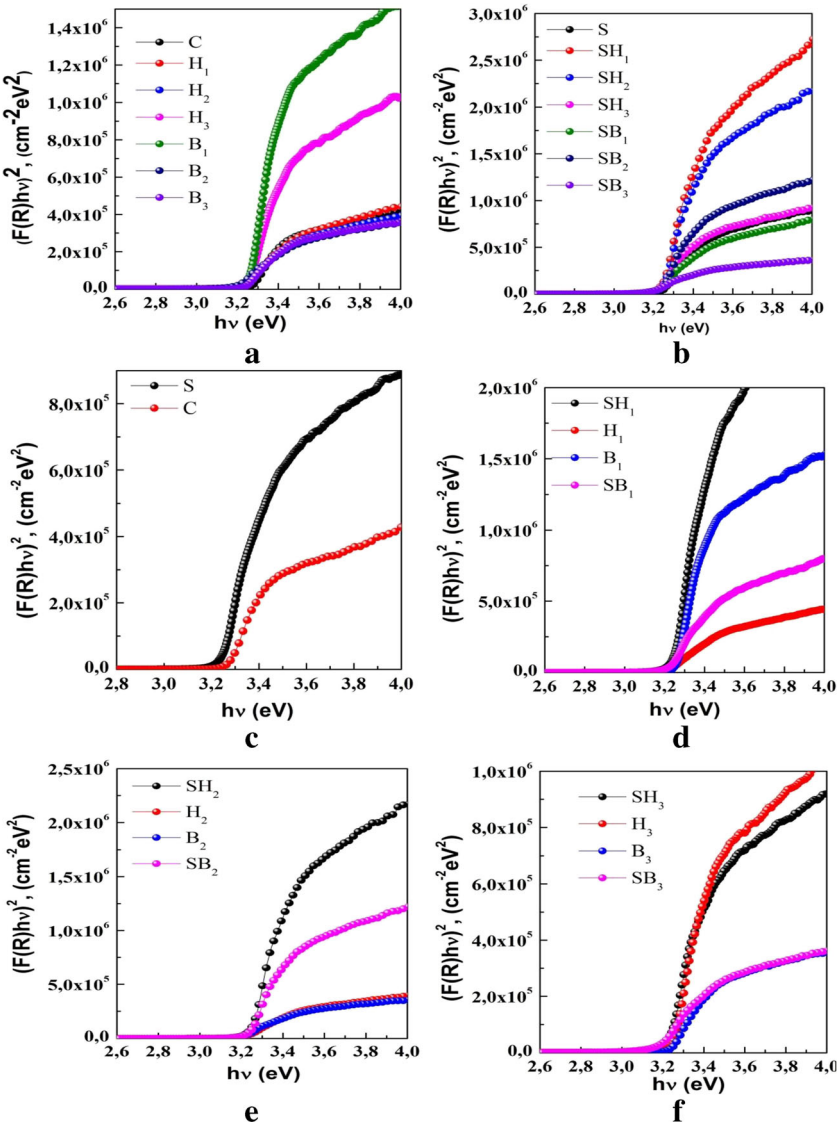

Fig. 6 **a**–**f** The plots of $(ah\upsilon)^2 \sim h\upsilon$ of **a** commercial ZnO matrix, **b** sol-gel ZnO matrix, **c** pure ZnO samples, **d** all nanocomposites having 0.1 wt% nanosheets, **e** all nanocomposites having 0.5 wt% nanosheets, **f** all nanocomposites having 1 wt% nanosheets

boundary resistance. It is reported that this structure may be useful for improving the performance of 2D device architectures.

Lewis et al. reinforced the graphene/h-BN pair as fillers to a polymer matrix. Graphene/h-BN reinforcement increased both the electrical conductivity and thermal conductivity of the matrix [36].

In recent years, although the number of studies investigating the effect of the synergistic effect of graphene/BNNS on various matrices has increased, the number of studies investigating the effect on semiconductor matrices such as ZnO is very few.

Conclusion

Nano-hybrid sheets of ZnO-doped graphene+boron nitride were synthesized using the exfoliation technique of the liquid phase. Details have been examined, and the electrical and optical properties of the materials have been determined. The nanosheets have the TEM pictures structure of both graphene and boron nitride. A combination of sheets and nano/micronutrients was found in the researched nanocomposite materials. A significant increase in electrical conductivity was observed in the reinforcement rate of 1 wt%. Only in the BN nanosheets and the reinforced samples increased reinforcement ratio and a decrease in electrical conductivity. The commercially ZnO matrix samples' electrical conductivity in terms of all dopant types and all reinforcement ratios was higher than the as-produced ZnO by the sol-gel method. The E_g values of the as-produced nanocomposites first decreased and then increased as the reinforcement ratio increased. The bandgap changing for all reinforcing types exhibit similar characters. For 0.1 wt% reinforcing, the bandgap value of ZnO decreases, but this value increases for 0.5 and 1 wt% reinforcing ratios. In 1 wt% reinforcing ratios, the bandgap

ratio is higher than 0.5 wt% reinforcing ratios. ZnO-doped graphene + boron nitride is a new promising nanocomposite for environmental, biomedical activities.

Funding This work is funded by the Deanship of Scientific Research at King Khalid University under grant number R.G.P.2/61/40.

Declarations

Competing interests The authors declare no competing interests.

References

1. Novoselov, K.S., Fal'ko, V.I., Colombo, L., Gellert, P.R., Schwab, M.G., Kim, K.: A roadmap for graphene. Nature. **490**(7419), 192–200 (2012)
2. Martinez, C., William, J., Herrera, H., Vinck-Posada, Paez, S.G.: Graphene-superconducting-graphene nanostructures for electron focusing. Optik. **197**, 163202 (2019)
3. Lu, Y., Cai, K., Li, Y., Duan, Z., Xi, Y., Wang, Z.: A high speed optical modulator based on graphene-on-graphene hybrid nanophotonic waveguide. Optik. **179**, 216–221 (2019)
4. Wu, Z., Li, X., Zhong, H., Zhang, S., Wang, P., Kim, T.H., Kwak, S.S., Liu, C., Chen, H., Kim, S.W., Lin, S.: Graphene/h-BN/ZnO van der Waals tunneling heterostructure based ultraviolet photodetector. Opt Express. **23**(15), 18864–18871 (2015)
5. Schwierz, F.: Graphene transistors. Nat Nanotechnol. **5**, 487–496 (2010)
6. Peplow, M.: Graphene: the quest for supercarbon. Nature. **503**, 327–329 (2013)
7. Du, A.: In silicon engineering of graphene-based van der Waals heterostructured nanohybrids for electronics and energy applications. Computatıonal Molecular Scİence. **6**(5), 551–570 (2016)
8. An, X., Liu, F., Jung, Y.J., Kar, S.: Tunable graphene-silicon heterojunctions for ultrasensitive photodetection. Nano Lett. **13**(3), 909–916 (2013)
9. Zhong, H., Xu, K., Liu, Z., Xu, G., Shi, L., Fan, Y., Wang, J., Ren, G., Yang, H.: Charge transport mechanisms of graphene/semiconductor Schottky barriers: a theoretical and experimental study. J Appl Phys. **115**, 013701 (2014)
10. Song, L., Ci, L., Lu, H., Sorokin, P.B., Jin, C., Ni, J., Kvashnin, A.G., Kvashnin, D.G., Lou, J., Yakobson, B.I., Ajayan, P.M.: Large scale growth and characterization of atomic hexagonal boron nitride layers. Nano Lett. **10**(8), 3209–3215 (2010)
11. Kim, K.K., Kim, S.M., Lee, Y.H.: A new horizon for hexagonal boron nitride film. J Korean Phys Soc. **64**(10), 1605–1616 (2014)
12. Meric. I, Petrone. N, Wang. L, Hone. J, Kim. P, Shepard. K.L, graphene field-effect transistors based on boron–nitride dielectrics, proceedings of the IEEE (2013)
13. Fu, X.L., Hu, Y.F., Yang, Y.G., Liu, W., Chen, S.F.: Ball milled h-BN: an efficient holestransfer promoter to enhance the photocatalytic performance of TiO_2. J HazardMater. **244**(245), 102–110 (2013)
14. Fu, X.L., Hu, Y.F., Zhang, T., Chen, S.F.: The role of ball milled h-BN in the enhanced photocatalytic activity: a study based on the model of ZnO. Appl Surf Sci. **280**, 828–835 (2013)
15. Song, Y., Xu, H., Wang, C., Chen, J., Yan, J., Xu, Y., Li, Y., Liu, C., Lia, H., Lei, Y.: Graphene-analogue boron nitride/Ag_3PO_4 composite for efficient visible-light-driven photocatalysis. RSC Adv. **4**, 56853–56862 (2014)
16. Choi, J., Reddy, D.A., Kim, T.K.: Enhanced photocatalytic activity and anti-photocorrosion of AgI nanostructures by coupling with graphene-analogue boron nitride nanosheets. Ceram Int. **41**, 13793–13803 (2015)
17. Güler, Ö., Güler, S.H.: Production of graphene-boron nitride hybrid nanosheets by liquid-phase exfoliation. Optik - International Journal for Light and Electron Optics. **127**(11), 4630–4634 (2016)
18. Güler, O., Güler, S.H., Taskin, M.: The production of graphene–boron nitride nanosheet heterostructures via liquid phase exfoliation assisted by a milling process. Bull Mater Sci. **42**(1), 1–7 (2019)
19. Güler, Ö., Güler, S.H., Selen, V., Albayrak, M.G., Evin, E.: Production of graphene layer by liquid-phase exfoliation with low sonication power and sonication time from synthesized expanded graphite. Fullerenes, Nanotubes and Carbon Nanostructures. **24**(2), 123–127 (2016)
20. Güler, S.H.: The production of boron nitride nanosheets using liquid-phase exfoliation assisted by ball milling process. Optoelectron Adv Mater. **12**(11-12), 754–758 (2018)
21. Guler, Ö.: Effect of carbon nanotubes produced by using different methods on electrical and optical properties of zinc oxide–carbon nanotube composite. Int J Mater Res. **106**(6), 641–646 (2015)
22. Guler. O, Guler. S.H, Yo. F, Aydin. H, Aydin. C, El-Tantawy. F, Duraia. E. M, Fouda. A.N, Electrical and optical properties of carbon nanotube hybrid zinc oxide nanocomposites prepared by ball mill technique, fullerenes, nanotubes and carbon nanostructures **23**, (2015), pp. 865–869
23. Guler, O.: The effect of an excessive amount of carbon nanotubes on the properties of zinc oxide-carbon nanotube nanocomposites. Sci Eng Compos Mater. **23**(4), 389–394 (2016)
24. Marinho, B., Ghislandi, M., Tkalya, E., Koning, C.E., With, G.: Electrical conductivity of compacts of graphene, multi-wall carbon nanotubes, carbon black, and graphite powder. Powder Technol. **221**, 351–358 (2012)
25. Ates, T., Tatar, C., Yakuphanoglu, F.: Preparation of semiconductor ZnO powders by sol–gel method: humidity sensors. Sensors Actuators A Phys. **190**, 153–160 (2013)
26. Zavadil, J., Kubliha, M., Kostka, P., Iovu, M., Labas, V., Ivanov, Z.G.: Investigation of electrical and optical properties of Ge-Ga-As-S glasses doped with rare-earth ions. J Non-Cryst Solids. **377**, 85–89 (2013)
27. Soltys, M., Gorny, A., Pisarska, J., Pisarski, W.A.: Electrical and optical properties of glasses and glass-ceramics. J Non-Cryst Solids. **498**, 352–363 (2018)
28. Güler, Ö., Güler, S.H., Başgöz, Ö., Albayrak, M.G., Yahia, I.S.: Synthesis and characterization of ZnO-reinforced with graphene nanolayer nanocomposites: electrical conductivity and optical band gap analysis. Materials Research Express. **6**(9), 095602 (2019)
29. Güler, S.H., Boyrazlı, M., Başgöz, Ö., Yakuphanoğlu, F.Y.: The effects of nanoporous Fe_2O_3 synthesized via mechano-thermal process on electrical and optical properties of zinc oxide. Phys B Condens Matter. **547**, 120–126 (2018)
30. Güler, S.H., Güler, Ö., Evin, E., Islak, S.: Electrical and optical properties of ZnO-milled Fe_2O_3 nanocomposites produced by powder metallurgy route. Optik. **127**(6), 3187–3191 (2016)
31. Abbasi, H.Y., Habib, A., Tanveer, M.: Synthesis and characterization of nanostructures of ZnO and ZnO/graphene composites for the application in hybrid solar cells. J Alloys Compd. **690**, 21–26 (2017)
32. Beura, R., Thangadura, P.: Structural, optical and photocatalytic properties of graphene-ZnO nanocomposites for varied compositions. J Phys Chem Solids. **102**, 168–177 (2017)
33. Liu, D., Zhang, M., Xie, W., Sun, L., Chen, Y., Lei, W.: Porous BN/TiO_2 hybrid nanosheets as highly efficient visible-light-driven photocatalysts. Appl Catal B Environ. **207**, 72–78 (2017)
34. Guo, F., Shen, X., Zhou, J., Liu, D., Zheng, Q., Yang, J., Jia, B., Lau, A.K.T., Kim, J.K.: Highly thermally conductive dielectric

nanocomposites with synergistic alignments of graphene and boron nitride nanosheets. Adv Funct Mater. **30**, 1910826 (2020)

35. Sajjad, M., Makarov, V., Mendoza, F., Sultan, M.S., Aldalbahi, A., Feng, P.X., Jadwisienczak, W.M., Weiner, B.R., Morell, G.: Synthesis, characterization and fabrication of graphene/boron nitride nanosheets heterostructure tunneling devices. Nanomaterials. **9**, 925 (2019)
36. Lewis, J.S., Barani, Z., Magana, A.S., Kargar, F., Balandin, A.A.: Thermal and electrical conductivity control in hybrid composites with graphene and boron nitride fillers. Mater Res Express. **6**, 085325 (2019)